

## Seasonal cycle of phytoplankton UV absorption at the Bermuda Atlantic Time-series Study (BATS) site

J. Ruairidh Morrison<sup>1</sup>

Woods Hole Oceanographic Institution, Woods Hole, Massachusetts 02543

Norman B. Nelson

ICESS, University of California Santa Barbara, Santa Barbara, California 93106

### Abstract

Measurements of the phytoplankton absorption coefficient,  $a_{ph}(\lambda)$ , at the Bermuda Atlantic Times-series Study (BATS) site demonstrated a seasonal pattern of absorption in the ultraviolet (UV) range. This was evidenced as peaks between 313 and 335 nm in  $a_{ph}(\lambda)$  from the surface waters (<50 m) in the summer months (April–October) that were smaller or absent in the winter (November–March). These peaks were most probably caused by pigments such as mycosporine-like amino acids. UV pigment expression in the surface samples, approximated from  $a_{ph}(319)/a_{ph}(365)$ , was linearly related to the irradiance exposure at 324 nm ( $r^2 = 0.81$ ). Irradiance exposure was estimated by a layered mixing model parameterized with the calculated mixed layer depth and modeled surface irradiance. Modeled UV irradiance, calculated with satellite-derived atmospheric data and an atmospheric radiative transfer model, was not significantly different from the measured monthly mean surface irradiance. These results suggest that UV pigments are potentially ubiquitous throughout the world's oceans and could be an important source of highly colored dissolved organic matter. A peak in the monthly averaged  $a_{CDOM}$  for both surface and deeper waters occurred during the period of maximal UV pigment expression at the surface, suggesting either a direct link or similar physical forcing of the two. UV pigments can also be important in higher trophic levels if bioaccumulation, which has been demonstrated in other regions, occurs.

Absorption of solar energy to drive photosynthesis exposes phytoplankton to potentially damaging ultraviolet (UV) radiation. Ultraviolet radiation incident on the earth's surface includes UV-A (315–400 nm) and UV-B (280–315 nm), but not UV-C (<280 nm) which is rapidly absorbed by oxygen and ozone in the modern day Earth atmosphere. Ozone also absorbs the majority of UV-B. The more energetic UV-B has the greatest potential for cell damage caused by both direct effects on DNA and proteins and indirect effects via the production of reactive oxygen species (*see review in Vincent and Neale 2000*). Recent research into the environmental effects of UV radiation has been stimulated by anthropogenic depletion of stratospheric ozone, most notably in the Antarctic (e.g., Karentz et al. 1991; Smith et al. 1992; Riegger and Robinson 1997; Neale et al. 1998b, c; Moisan and Mitchell 2001). To date, little work has been done on the biological effects of UV radiation in the clear waters of oligotrophic oceans at lower latitudes, where the UV flux can

be seasonally variable and an order of magnitude greater than at the poles (Whitehead et al. 2000).

Lower levels of atmospheric oxygen in earlier geological times most likely selected for species able to produce UV-screening compounds (Cockell and Knowland 1999; Roze-ma et al. 2002). Mycosporine-like amino acids (MAAs) are UV absorbing, or sunscreens, compounds that contain either an aminocylcohexenone or aminocylcohexenimine unit. MAAs are widespread in the marine environment, from the poles to the tropics, and occur in a large number of taxa including bacteria, cyanobacteria, algae, invertebrates, and vertebrates (e.g., Shick and Dunlap 2002). Synthesis of MAAs is proposed to occur via the shikimate pathway, a catabolic and synthetic pathway not present in animals. The lack of biosynthetic ability in animals leads to the assumption that bioaccumulation accounts for MAA presence in both invertebrates and vertebrates. Near-ubiquitous MAA presence across taxonomic levels suggests an early origin and continued importance (*see reviews in Bandaranayake 1998; Cockell and Knowland 1999; Shick and Dunlap 2002*).

Approximately 19 MAAs are known to occur in the marine environment with absorption peaks between 310 and 360 nm, a combination of which can lead to a broad absorption waveband in the UV (Cockell and Knowland 1999). MAAs have been documented in a wide number of phytoplankton (Vernet and Whitehead 1996; Riegger and Robinson 1997; Hannach and Sigleo 1998; Neale et al. 1998a; Moisan and Mitchell 2001; Laurion et al. 2002) including *Trichodesmium* sp. (Subramaniam et al. 1999) and toxic bloom-forming species. In phytoplankton, MAAs have been shown to be effective sunscreens (Garcia-Pichel 1994; Neale et al. 1998a) that are inducible by solar radiation. MAA

<sup>1</sup> Present address: OPAL, University of New Hampshire, Durham, New Hampshire 03824.

### Acknowledgments

We thank all the people associated with the data collection, the BBOP and BATS technicians, and the crew of the R/V *Weatherbird II*. Jed Goldstone also provided much support, as did Heidi Sosik. This work was partially supported by the NASA SIMBIOS contracts NAS5-00198 and NAS5-00200. The MODIS atmospheric data used in this study were acquired as part of NASA's Earth Science Enterprise. The algorithms were developed by the MODIS science teams. The data were processed by the MODIS adaptive processing system (MODAPS) and Goddard Distributed Active Archive Center (DAAC) and are archived and distributed by the Goddard DAAC. This is WHOI contribution 10879.

induction exhibits wavelength dependence (Hannach and Sigleo 1998; Klisch and Hader 2002) and a dose–magnitude response (Riegger and Robinson 1997; Moisan and Mitchell 2001). In addition, Klisch and Hader (2000) observed an alteration of MAA composition with spectral irradiance composition. Diel variability in MAA induction has been demonstrated in cyanobacteria (Shina et al. 2001). Once induced, MAAs seem to be conserved with cellular levels reduced only on cell division (Riegger and Robinson 1997).

UV radiation has been shown to inhibit photosynthesis in natural phytoplankton assemblages (e.g., Smith et al. 1980), and this inhibition has been investigated in the context of vertical mixing (Cullen and Lesser 1991; Smith et al. 1992; Neale et al. 1998c). Phytoplankton from regions with shallower mixing depths tend to show an enhanced tolerance to UV, suggesting acclimation with higher UV exposure (Neale et al. 1998b), possibly caused by increased UV screening compounds. Both seasonal and depth-dependent changes in MAA concentrations have been observed in benthic organisms, presumably resulting from varying UV exposure (*see review in Shick and Dunlap 2002*). In freshwater zooplankton, the concentration of MAAs has been related to UV radiation exposure (Tartarotti et al. 2001).

MAAs have been shown to be released from phytoplankton grown in cultures (Vernet and Whitehead 1996) and have been identified in colored (or chromophoric) dissolved organic matter (CDOM) of coastal waters, where they might contribute up to 10% of the CDOM absorption at 330 nm (Whitehead and Vernet 2000). Initial evidence suggests that MAAs are only slowly lost from the DOM pool, as evidenced by low photodegradation rates in culture filtrates (Vernet and Whitehead 1996) and by continued MAA presence in coastal waters ~2 weeks after a peak in the particulate fraction (Whitehead and Vernet 2000). Because of the small contribution of terrestrial inputs to CDOM in oceanic waters, the MAA contribution to the total CDOM absorption spectrum may be increased.

Although compounds that absorb in the UV might not be considered pigments in the classical sense (they do not absorb in the visible spectral region and are therefore not colored to the human eye), they are functionally indistinct from them and might even appear “colored” to organisms with vision in the UV. Similarly, UV-absorbing DOM might not be classically considered colored or even chromophoric, which indicates the ability to bear color (Simpson and Weiner 1989). The terms pigment and colored in this paper have been extended to include those compounds that absorb in the UV.

Here, we present time-series data collected at the Bermuda Atlantic Time-series Study (BATS) site over a period of two and a half years that demonstrates seasonal production of UV pigments in phytoplankton. We examine the roles of incident UV irradiance and mixing depth in controlling UV pigment production and explore possible relationships between UV pigment production and CDOM. The importance of bioaccumulation of UV pigments by higher trophic levels is also explored.

## Methods

*Water sampling*—Sample water was collected from the BATS site (31°40'N, 64°10'W). Samples were collected from the R/V *Weatherbird II* via Niskin bottles equipped with epoxy-coated springs on a conductivity, temperature, and depth (CTD) rosette (Knap et al. 1997). Samples for CDOM spectroscopy were filtered with an acid-washed all-glass filtration unit through 0.2- $\mu\text{m}$  Nuclepore filters that had been prerinsed with 500 ml of Milli-Q (Millipore) water. Filtered samples were stored in acid-washed dark glass bottles (Qorpak) with Teflon (PTFE)-lined lids in the dark at 4°C until analysis (Mitchell et al. 2000). Samples for particle absorption (~4 liters) were collected in dark Nalgene bottles and filtered onto 25-mm-diameter Whatman GF/F glass fiber filters, and the filters were immediately frozen in liquid nitrogen until analysis.

*Absorption spectroscopy*—All CDOM spectroscopy was performed with a Perkin-Elmer Lambda 18 spectrophotometer and matched 10-cm quartz-windowed cuvettes. Specifications of the instrument and practical experience with its use have indicated that we can accurately measure absorption coefficients of filtered seawater down to 0.03  $\text{m}^{-1}$ , which typically occurs between 380 and 420 nm in natural samples (Nelson et al. 1998). The instrument was zeroed with Milli-Q water in both cuvettes, and all measurements were made with sample and reference at room temperature. The spectra were acquired as decadal optical density, corrected for baseline offsets (e.g., Green and Blough 1994) and were converted to absorption coefficients ( $\text{m}^{-1}$ ) by converting to base  $e$  (multiplying by 2.303) and dividing by the geometric path length (0.1 m).

Particulate absorption was estimated with the quantitative filter technique (QFT, Mitchell 1990; Mitchell et al. 2000). Absorption spectra of the loaded filter pads were made on the Lambda 18 spectrophotometer equipped with a scattered transmission accessory. Baseline effects were removed by subtracting the spectrum of a blank GF/F filter from the same box that had been wetted with filtered seawater. These baseline-subtracted optical density spectra were then corrected for the pathlength amplification effect (beta correction), following Mitchell (1990) and Cleveland and Weidemann (1993), resulting in an estimate for the spectral particulate absorption coefficient spectrum,  $a_p(\lambda)$ . Coefficients for the beta correction were determined as described in Nelson et al. (1998) according to the methods described by Mitchell (1990) and Cleveland and Weidemann (1993). We did not sample *Trichodesmium* colonies because their large scale and sparse abundance at the BATS latitude (Orcutt et al. 2001) precludes accurate quantification of their light absorption properties by the QFT method. Pathlength amplification of *Trichodesmium* colonies collected on filters has also not been studied. Colonies rarely appeared on filters (possibly because of buoyancy within the Niskin bottles), and when they did, filters were oriented so the light beams passed through a different portion of the filter. We did not observe the characteristic visible light absorption signature of *Trichodesmium* (Subramaniam et al. 1999) in our data set, further suggesting that loose trichomes (i.e., *Trichodesmium* fil-

Table 1. Parameterization of the MODIS-SBDART model with MODIS scientific dataset means, the SBDART INPUT file parameters, and the means and standard deviations. The aerosol parameters (TBAER, GBAER, and ABAER) have 114 data points because two values were missing. The rest of the parameters have 116 values.

MODIS SDS Name	SBDART	Mean (SD)	Units
Total_Ozone_Mean_Mean	UO3	0.273(0.011)	atm cm $\equiv$ 1,000 Dobson units
Atmospheric_Water_Vapor_Mean_Mean	UW	3.31(0.53)	g cm <sup>-2</sup> $\equiv$ cm
Cloud_Optical_Thickness_Combined_Mean_Mean	TLOUD	6.54(4.42)	—
Cloud_Effective_Radius_Combined_Mean_Mean	NRE	26.24(3.00)	$\mu$ m
Effective_Optical_Depth_Average_Ocean_Mean_Mean	TBAER	0.0819(0.0399)	—
Asymmetry_Factor_Average_Ocean_Mean_Mean	GBAER	0.738(0.028)	—
Angstrom_Exponent_2_Ocean_Mean_Mean	ABAER	0.197(0.227)	—

aments free of colonies) were not important contributors to particulate absorption in our sample set.

Detrital particulate absorption was estimated after extracting phytoplankton pigments from the filters used to determine  $a_p(\lambda)$  with absolute methanol (e.g., Mitchell et al. 2000). Filters were extracted for a minimum of 4 h at room temperature, but occasional samples from the subsurface chlorophyll maximum layer resisted extraction, as was apparent from absorption spectra of the filters, which exhibited peaks due to phytoplankton pigments at 440 and 675 nm. These samples were extracted for up to 18 h in order to remove the residual peaks. This procedure results in an estimate of the detrital particle absorption coefficient spectrum,  $a_d(\lambda)$ . The phytoplankton absorption spectrum,  $a_{ph}(\lambda)$ , can be determined from the difference between  $a_p(\lambda)$  and  $a_d(\lambda)$  [ $a_{ph}(\lambda) = a_p(\lambda) - a_d(\lambda)$ ].

**Spectral irradiance**—Vector downwelling irradiance ( $E_d$ ,  $\mu$ W cm<sup>-2</sup> nm<sup>-1</sup>) was measured by Satlantic multichannel radiometers (SPMR, profiler; SMSR, surface logger, located  $\sim$ 10 m above the sea surface). The radiometer wavelength bands were centered near 324, 340, 379, 411, 443, 490, 510, 555, 565, 665, and 683 nm. The SPMR was deployed from the vessel's fantail on a free-fall, hand recover basis. The hand deployment procedure is used to offset the ship shadow influence and allow for a slow (sinking rate  $\sim$ 1 m s<sup>-1</sup>) profile. The in-water data were processed and quality control was applied using guidelines established by the Bermuda Bio-Optics Project (Siegel et al. 1995). Diffuse attenuation coefficients ( $K_d$ , m<sup>-1</sup>) were determined from linear regressions of the log-transformed irradiance profiles (Siegel and Dickey 1987). Midday surface UV irradiance values,  $E_s(\lambda)$ , were estimated from SMSR data as the mean observed during the SPMR profile with the maximum mean daily  $E_s(324)$ . Only profiles measured within  $\pm$ 2.4 h of midday were used in determining the midday surface irradiance values.

We also predicted midday surface irradiances for the BATS site from the plane-parallel Santa Barbara DISORT atmospheric radiative transfer (SBDART) model (Ricchiuzzi et al. 1998). Atmospheric aerosols, ozone, and clouds are important in predicting UV irradiances by radiative transfer models (e.g., Krotkov et al. 2001; Vasilkov et al. 2001). SBDART was parameterized with products from the Level 3 8-d Moderate Resolution Imaging Spectroradiometer (MODIS) atmosphere global joint product (MOD08\_E3),

which has a spatial resolution of 1° ([http://modis-atmos.gsfc.nasa.gov/MOD08\\_E3/index.html](http://modis-atmos.gsfc.nasa.gov/MOD08_E3/index.html)). In total, 116 MODIS files, including both collection 003 and 004 files, were available spanning 18 Feb 2000 to 4 Jan 2003. There was no MODIS data available at the time of processing between 17 Jun and 31 Oct 2000. For each image, the model was initialized with the day of year, latitude, and longitude, and with MODIS-derived values, including, (1) the integrated water vapor amount (cm  $\equiv$  g cm<sup>-2</sup>), (2) integrated ozone concentration (atm cm = 1,000 Dobson units), (3) clouds described from the combined optical thickness (all cloud phases) for the ocean at 550 nm and the cloud effective drop radius ( $\mu$ m), and (4) aerosols from the effective average optical depth for the ocean at 550 nm, the asymmetry factor for the ocean, and the angstrom exponent (Table 1). The aerosol single scattering albedo was set to 0.9, and the SBDART model seawater surface albedo and tropical atmosphere were used.

**Irradiance-mixing model**—We examined the relationship between irradiance exposure and the degree of UV pigment expression with a simple multilayer irradiance-mixing model, which is similar to the single- and three-layer models described by Neale et al. (1998c). The model assumes that mixing only occurs in the surface mixed layer (SML) (i.e., those depths above the mixed layer depth [MLD]) and that mixing below this layer is negligible. The mixed layer depth was calculated from CTD profiles.

The simplest case is a single layer that results in complete mixing of the SML each day. For this single-layer model, the midday irradiance levels are calculated at 1-m depth intervals by propagating the daily surface irradiance to depth. Propagation is achieved with an exponentially decreasing function and assuming  $K_d(\lambda)$  is constant with depth.

$$E_d(\lambda, z) = E_d(\lambda, 0^-)e^{-K_d(\lambda)z} \quad (1)$$

We assumed that irradiance exposure in a completely mixed layer is independent of depth and that total exposure within a layer should be the same both before and after mixing. Therefore, single-layer mixing can be simulated by setting the exposure at all depths in the SML equal to the mean irradiance in the layer. Below the MLD, the irradiance exposure is simply the irradiance propagated to depth according to Eq. 1. We calculated irradiance exposure for each day

with the mixing model and inputs of incident irradiance, attenuation coefficient, and MLD.

To examine the effects of decreased mixing with depth in the SML, multilayer models were used to approximate decreased mixing with depth. The SML is split into layers of equal vertical thickness. For a system with  $n$  layers, the daily  $E_d(\lambda, z)$  is divided into  $n$  equal fractions that are mixed differently. For each day, mixing is simulated as  $n$  events. The initial mixing event mixes the first irradiance fraction over the whole SML (i.e., each layer receives the same exposure from the first irradiance fraction, and this exposure is equal to the mean irradiance over the SML). The next event mixes the irradiance fraction in the top  $n - 1$  layers, and this is repeated with one less layer until just the top layer is mixed in the last event. In layers that are not mixed during an event, the fractional irradiance exposure is just the fractional irradiance propagated to depth. Finally, the total midday irradiance exposure at each depth is calculated as the sum of the fractional irradiance exposure.

For the example of a two-layer model,  $E_d(\lambda, z)$  is divided in half. The initial mixing event mixes one half of the irradiance over the entire SML (or both layers). Below the MLD, the fractional irradiance exposure is just the fractional irradiance propagated to depth. The next mixing event mixes the second half of the irradiance over the top layer. During this second mixing event, all depths below the top layer, receive half the irradiance propagated to depth with Eq. 1. The total irradiance exposure profile is the sum of the profiles of the mixed fractional irradiance exposure.

UV pigment expression was also modeled on the basis of the irradiance exposure model; this required relationships for both the rates of production and loss of pigment expression. Little is known about the rate of decrease in the concentration of UV-absorbing pigments in phytoplankton. Initial evidence suggests that UV pigments are conserved with cellular levels reduced only on cell division (Riegger and Robinson 1997). The lack of knowledge of these rates necessitated some simple assumptions. These assumptions were that (1) at the cellular level, UV pigment expression decreases with cell division by a factor of two, (2) cell division occurs once per day, and (3) the UV pigment expressions were the same on days preceding observations. The daily increase in peak expression would then be half the observed pigment expression. In the absence of UV exposure, expression would decrease by half.

## Results

**Observations**—Phytoplankton in surface samples (<50 m) in the summer (April–October) demonstrated distinct absorbing bands in the UV, which were absent or much lower in concentration in the winter (November–March, Fig. 1). The presence of UV-absorbing pigments was inferred from the absorbing bands. The effect of these pigments was observed as peaks in the absorption at  $\sim 319$  nm and minima at  $\sim 365$  nm, which were present in the summer and absent in the winter. The wavelength of maximum absorption was not constant but instead varied from  $\sim 313$  to  $\sim 335$  nm. The UV pigment expression, as indicated by the relative UV pig-

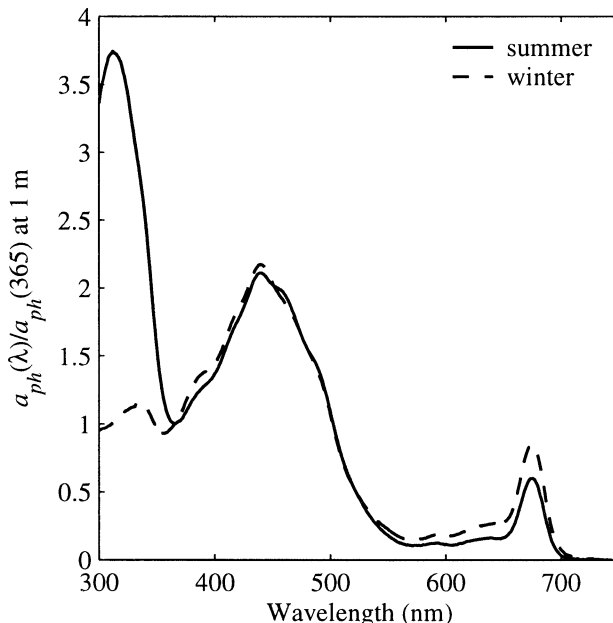


Fig. 1. Example surface water phytoplankton absorption spectra normalized to  $a_{ph}(365)$ . The summer spectrum shows high absorption in the UV that is typically associated with Mycosporine-like amino acids.

ment peak height,  $a_{ph}(319)/a_{ph}(365)$ , showed distinct variation with both time of year and depth (Fig. 2A). This relationship was suggestive of higher relative peak height with higher UV radiation exposure. The ratio of phytoplankton absorption at the main peaks of chlorophyll absorption,  $a_{ph}(440)/a_{ph}(675)$ , also showed a depth-dependent seasonal variation with higher values at the surface in the summer (Fig. 2B). Differences in blue-to-red ratio can be caused by differences in accessory pigment concentrations and variations in the packaging effect caused by cell size and cellular pigment concentrations (e.g., Morel and Bricaud 1981; Bricaud et al. 1983). The variation in both the UV pigment expression and the blue-to-red ratio was minimal at depths  $>60$  m. Phytoplankton biomass, as indicated by the proxy  $a_{ph}(440)$ , also showed a seasonal cycle, with a spring phytoplankton increase, followed by decreased levels in surface waters and development of subsurface maxima (Fig. 2C). This was consistent with previous reports for the BATS site (e.g., Steinberg et al. 2001). The seasonal cycle of absorption by CDOM was more complex, with what appeared to be an initial increase each year at most depths following the spring phytoplankton increase and coincident with the onset of UV pigment expression (Fig. 2D). After the spring, increase in  $a_{CDOM}$  levels in surface waters were generally less than those in deeper water, which is consistent with previously published data (Nelson et al. 1998; Nelson and Siegel 2002). Mean  $a_{CDOM}(324 \text{ nm})$  was  $0.138 \text{ m}^{-1}$  ( $\sigma = 0.049$ ,  $N = 267$ ), mean  $a_{ph}(324)$  was  $0.0035 \text{ m}^{-1}$  ( $\sigma = 0.0021$ ,  $n = 268$ ), and mean  $a_{ph}(440)$  was  $0.067 \text{ m}^{-1}$  ( $\sigma = 0.0040$ ,  $n = 268$ ). Chlorophyll concentrations ranged from  $0.002$  to  $0.606 \text{ mg m}^{-3}$ , with a mean of  $0.1519 \text{ mg m}^{-3}$  ( $\sigma = 0.113$ ,  $n = 245$ ).

Mixed layer depth varied both seasonally and interannually and was similar to values reported previously (e.g.,

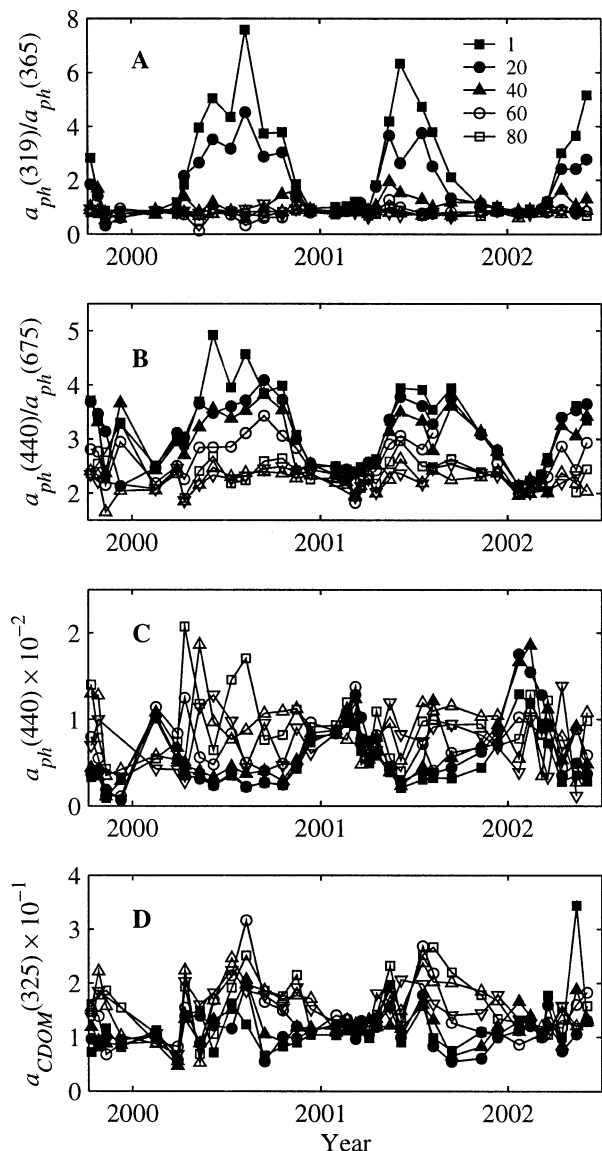


Fig. 2. Seasonal and interannual variations in phytoplankton and CDOM absorption at the BATS site. (A) Relative UV pigment peak height  $a_{ph}(319)/a_{ph}(365)$  showed maxima in surface waters during the summer. (B) Blue-to-red ratio of phytoplankton absorption,  $a_{ph}(440)/a_{ph}(675)$ , at the chlorophyll  $a$  absorption maxima showed higher values in the summer at the surface. (C)  $a_{ph}(440)$  showed a spring increase. (D)  $a_{CDOM}(325)$  showed two annual increases in 2000 and 2001, one after the spring phytoplankton increase and at the initial increase in the UV pigments and the other in the summer coincident with maximal UV pigment expression.

Steinberg et al. 2001; Fig. 3A). A seasonal pattern was also discernible in the downwelling attenuation in the UV, with highest values between November and May (Fig. 3B). The monthly mean  $K_d(324)$  at 10 m was significantly related to the  $a_{ph}(440)$  at 20 m ( $F$ -test,  $n = 22$ ,  $P < 0.001$ ). There were no other significant relationships of  $K_d(324)$  with the measured absorptions at 324 nm, including the total absorption coefficient. The magnitudes of the attenuation coefficients are similar to previous measurements in the Sargasso Sea (Smith and Baker 1979). Midday surface irradiance in the

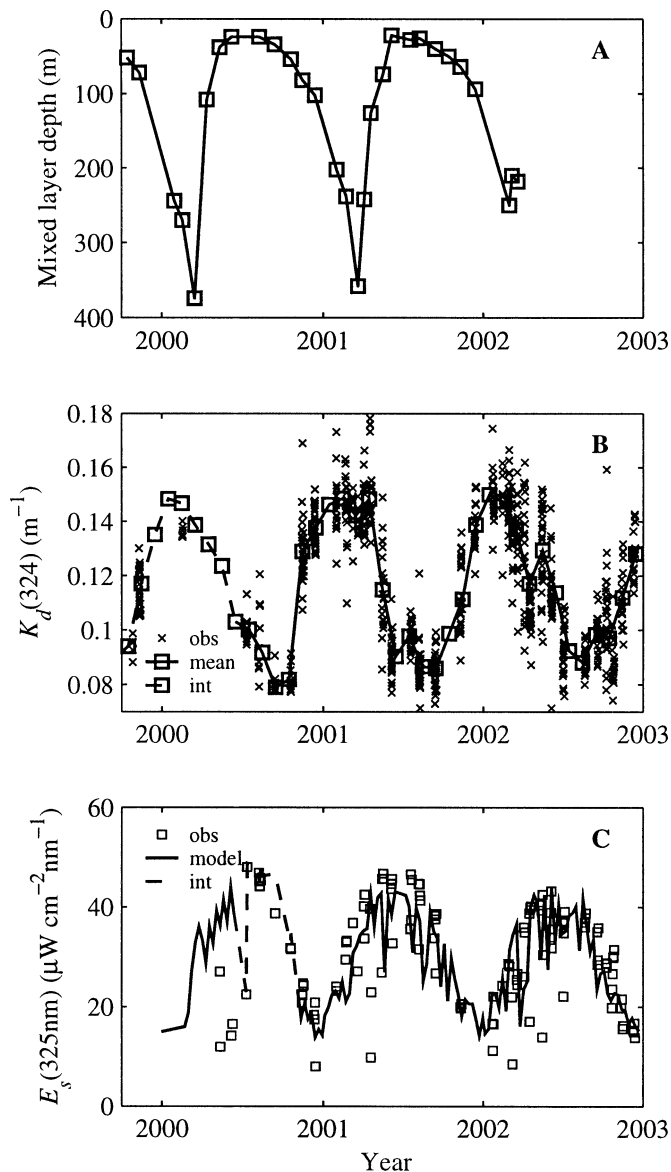


Fig. 3. Seasonal and interannual variation in the principal parameters controlling the underwater UV radiation. (A) Mixed layer depth calculated from BATS CTD cast data. (B)  $K_d(324)$  at 10 m showing both individual observations and monthly means. Scarcity of individual observations prior to 2 Jul 2000 lead to mean values before being derived from annual monthly means. (C) Surface irradiance from the MODIS-SBDART model and the BBOP reference radiometer. Modeled data between 13 Jun and 4 Nov 2000 are not available because of lack of satellite data. Differences between measured and modeled values could be a result of differences in sample time, errors inherent in the model parameterization, instrument calibration, or a combination of factors.

UV showed a distinct seasonal cycle both in the values observed at the BATS site with the surface reference radiometer and those predicted by the MODIS-SBDART model (Fig. 3C). Monthly means were calculated in an attempt to remove some of the temporal variability associated with the sampling of the two surface irradiance values. There were significant relationships for all three SMSR UV wavelengths

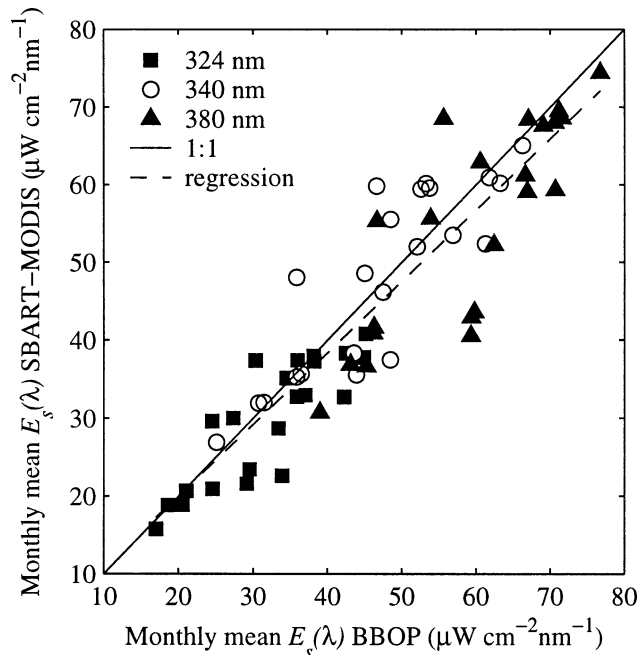


Fig. 4. Comparison of the BBOP and MODIS-SBDART mean monthly UV irradiances. For each wavelength, there was a relationship not significantly different from 1:1 (Table 2).

(324, 340, 380 nm) and for the combination of all three wavelengths with these monthly means. These relationships were not significantly different from 1:1 (Table 2; Fig. 4).

**Modeling**—The multilayer irradiance–mixing model was parameterized with observed mixed layer depths, the MODIS-SBDART midday  $E_s(325)$  supplemented with field observations between 13 Jun 2000 and 04 Nov 2000, and monthly mean  $K_d(324)$ . Values of MLD,  $E_s(325)$ , and  $K_d(324)$  were linearly interpolated to give daily values, and the mixing model was run from 31 Dec 1999 for 800 days with one, two, and three layers. The expression of the UV pigments was quantified as the relative UV peak height minus the mean relative peak height at the minimum depth of zero expression, effectively 80 m. This quantification meant that UV pigment expression was effectively zero in the absence of UV pigments. The maximum correlation between the 81 observed UV pigment expressions and the modeled irradiance dose for depths <50 m was with a two-layer model ( $r = 0.90$ ). Only depths <50 m were used for the correlation because at depths greater than 50 m, the UV pigment expression was minimal. For one- and three-layer models, the correlation coefficient was 0.85 and 0.86, respectively. As an initial approximation, linear regression was used to parameterize the relationship between the midday irradiance exposure and the UV pigment expression (Fig. 5). The intercept of this regression was not significantly different from zero ( $t = -0.33$ ,  $P = 0.75$ ).

The UV pigment expression was modeled with the irradiance–mixing model, and the rates of increase and loss of UV pigments were calculated on the basis of the assumptions described previously. The daily irradiance exposure–dependent rate of increase, derived from the expression–ir-

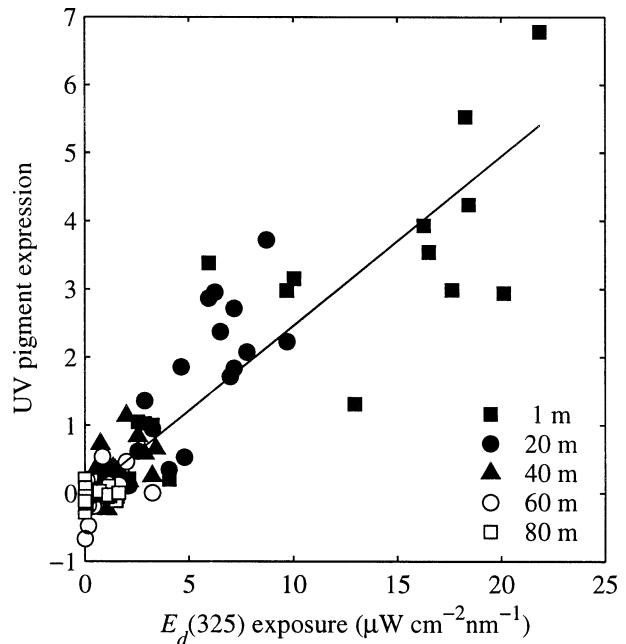


Fig. 5. Observed UV pigment expression and modeled irradiance exposure from the irradiance mixing model with two layers. There was a significant relationship between the two for depths <50 m where there was detectable pigment expression (expression =  $0.250 \times$  exposure  $- 0.030$ ,  $r^2 = 0.81$ ,  $F = 347$ ,  $P < 0.01$ ).

radiance relationship, was  $0.125 (\mu\text{W cm}^{-2} \text{ nm}^{-1})^{-1} \text{ d}^{-1}$ . Each night, the pigment expression was halved. The model was run with the interpolated environmental variables for 800 d starting on 31 Dec 1999. The initial UV pigment expression was set to 0.1. Despite the simplicity of this model, there was both qualitative and quantitative agreement between the modeled and observed UV pigment expression (Fig. 6A,B). The modeled expression explained 81% of the variance in the observed data.

## Discussion

We have documented seasonal induction of enhanced UV absorption by phytoplankton in the summer stratified surface waters of the Sargasso Sea. The spectral characteristics are consistent with previously reported UV-absorbing compounds, most probably MAAs, and the variation in the wavelength of maximal absorption suggests wavelength-specific induction (Klisch and Hader 2002; Krabs et al. 2002). The ability to produce or use UV-absorbing compounds is thought to have been important early in the development of life on earth (Cockell and Knowland 1999). The present day ubiquitousness of these pigments across taxa and geographical regions has been previously documented, indicating the continued importance of UV-absorbing pigments. To our knowledge, our results are the first to show a multiyear seasonal cycle in UV-absorbing pigments in phytoplankton.

It should be noted that use of the QFT to measure phytoplankton absorption limits the spectral range to wavelengths >300 nm because of the low transmittance of GF/F filters below this wavelength. Use of alternative techniques

Table 2. Linear regression results for the comparison of the monthly mean BBOP and SBDART-MODIS predicted UV irradiances. There were significant relationships at all wavelengths, and the fitted lines were not significantly different from 1:1.

$\lambda$ (nm)	Intercept (nm)	SE	$t$	$P$	Slope	SE	$t$	$P$	$r^2$	$F$	$P$
324	4.57	3.61	1.27	0.22	0.78	0.11	1.98	0.06	0.72	51.71	<0.01
340	6.60	5.92	1.12	0.28	0.88	0.12	1.01	0.32	0.72	51.70	<0.01
380	-2.85	9.31	-0.31	0.76	0.97	0.15	0.19	0.85	0.66	39.67	<0.01
All	1.97	2.57	0.77	0.45	0.91	0.05	1.65	0.10	0.82	299.65	<0.01

such as particle transfer to quartz slides (Allali et al. 1995) might avoid these limitations.

The observed seasonal cycle in relative UV absorption might be a result of photoacclimation to change in daily UV exposure by the existing phytoplankton crop. Alternatively, the cycle could result from seasonal succession of phytoplankton with UV-absorbing pigment expression. It is also possible that both of these explanations contribute. The UV absorption peak is at its largest relative value during the summer, when a shift in community structure typically occurs to a predominantly prokaryotic picoplankton community from a community with a larger relative population of flagellates such as prymnesiophytes and pelagophytes (Anderson et al. 1996; Steinberg et al. 2001). Induction of MAA synthesis has been demonstrated in prymnesiophyte species (Moisan and Mitchell 2001), and UV-absorbing compounds are known to be present in the cyanobacterium *Trichodesmium* spp. (Subramaniam et al. 1999). With available data, it is not possible to determine whether photoacclimation or species succession is more important.

Assuming the *Trichodesmium* colony population has not been sampled by our methods (a valid assumption because colonies are easily observed on filters) and trichome abundances are small at this site (Orcutt et al. 2001), we are observing the spectra of primarily unicellular picoplankton and nanoplankton. This result argues against the sunscreen model of (Garcia-Pichel 1994), which indicates that microbes in the microplankton size range ( $\sim 10 \mu\text{m}$  and greater) can use internal pigments as effective sunscreens whereas the picoplankton ( $< 1 \mu\text{m}$ ) cannot, and the nanoplankton ( $1\text{--}10 \mu\text{m}$ ) can do so but with much lower efficiency than larger cells. Because the surface summertime population at the BATS site is dominated by picoplankton (DuRand et al. 2001), our results suggest that these organisms are using MAAs as effective sunscreen.

Despite complications associated with temporal and spatial sampling differences, there was good agreement between the UV irradiances estimated by SBDART with inputs from MODIS atmospheric data and those observed in situ (Figs. 3C, 4). Some of the temporal differences could be minimized by decreasing the sampling differences, for example by using daily MODIS products with greater spatial resolution (Level 2). This approach for modeling surface UV irradiance has great potential for future work, both photochemical and biological, because of the ease of acquisition of both the SBDART model and the MODIS atmosphere products.

In the Sargasso Sea, the absorption of CDOM dominates in the UV. This has led to the assumption that CDOM is

the major determinant of UV light availability (Siegel et al. 2002). In contradiction to this assumption, the seasonal cycle of UV attenuation at 10 m appears to be in phase with phytoplankton biomass but no other measured absorptions (Figs. 2, 3). This covariance suggests that phytoplankton, or some other unmeasured factor covarying with them, are the primary contributors to the annual variation of UV attenuation in the Sargasso Sea. An increased contribution of phytoplankton scattering to attenuation and seasonal variation of the solar zenith angle could be a possible explanation for this phenomenon. These results highlight the need for more detailed investigations of the factors determining the variability of UV radiation transmission into the world's oceans.

Despite its simplicity, the irradiance-mixing model for phytoplankton UV pigment expression worked well when initialized with the MODIS-SBDART estimated surface UV irradiances. An approximately linear increase in UV pigment expression with irradiance exposure was observed (Fig. 5), in keeping with previous observations on algal cultures (Riegger and Robinson 1997; Moisan and Mitchell 2001). This is the first time UV pigment expression dependent on radiation exposure has been demonstrated for natural phytoplankton assemblages from oligotrophic waters.

Modeled UV pigment expression was significantly related to that observed (Fig. 6). The close link with the pigment expression-irradiance exposure relationship was indicated by the similar variances explained by the linear regressions. The model was limited by the current poor understanding of the kinetics of UV pigment induction and loss. Induction in Antarctic phytoplankton cultures required constant illumination and has been shown to follow an initial lag phase (10 to 24 h), an exponential phase (60 to 120 h), and then a steady-state phase (Riegger and Robinson 1997). This induction lag was not included in the model because of the constant nature and smaller magnitude of the irradiances of the previous study in comparison to those at the BATS site. To date, no work has been done on the loss of UV pigment expression. Although there is evidence for phased diel cell division of phytoplankton, both in cultures of isolates from the Sargasso Sea and in situ (DuRand and Olson 1996; DuRand et al. 2002), the effect on the intracellular concentration of UV-absorbing pigments is unknown. Cultures of cyanobacteria exposed to natural solar radiation exhibited a diel pattern in MAA induction; peak area increased in the light phase and slightly decreased in the dark phase, but the timing of cell division was not determined (Shina et al. 2001). A more detailed model including depth-dependent attenuation, spectral irradiance, and more realistic phytoplank-

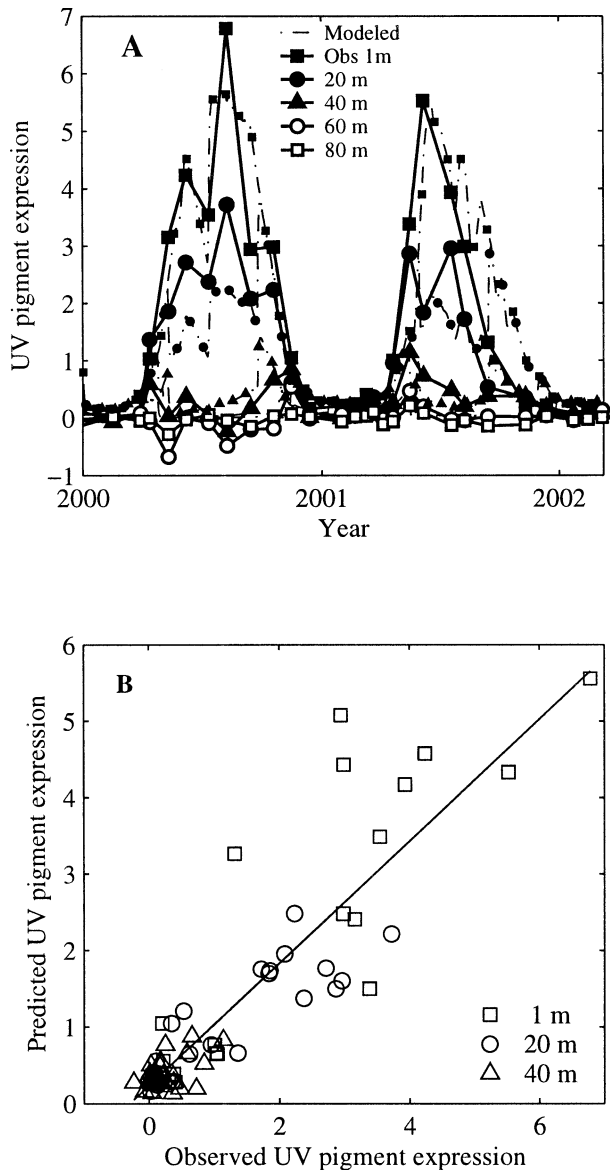


Fig. 6. Comparison of the predicted and observed UV pigment expression (relative peak height – mean relative peak height at 80 m) at the BATS site. (A) The modeled and the observed UV pigment expression with time. There was good agreement between the two with the modeled results (thin lines and small symbols) showing similar trends to the observed results (thick lines and larger symbols). (B) The predicted UV pigment expression was significantly related to that observed for the top three depths (predicted =  $0.80 \times$  observed + 0.23,  $r^2 = 0.81$ ,  $F = 343$ ,  $n = 81$ ,  $P < 0.01$ ).

ton growth parameters coupled to a more complex physical mixing model might explain more of the variability in the observed UV pigment expression. Our results suggest a mechanism to explain previous observations of differential sensitivity of photosynthesis in waters with similar surface UV irradiance conditions but with varied mixed layer depths (Neale et al. 1998b).

The sources of CDOM in the open ocean remain uncharacterized, but bacterial remediation of DOM is thought to be the major source (Nelson et al. 1998; Nelson and Siegel

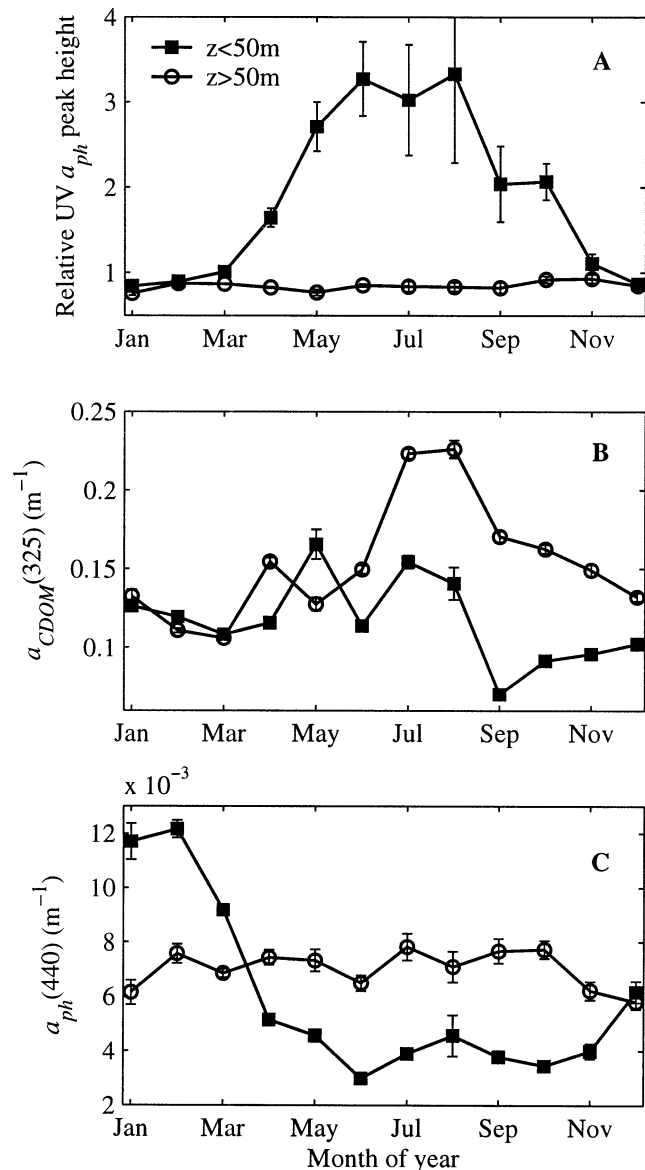


Fig. 7. Monthly climatology of (A) the relative UV pigment peak, (B) CDOM absorption at 325 nm, and (C) phytoplankton absorption at 440 nm for surface (<50 m) and deeper (>50 m) waters from data presented in Fig. 2. UV pigment expression is evident in surface waters during the summer months and absent in deeper waters. The peak CDOM levels in both surface and deeper waters were out of phase with phytoplankton biomass, as indicated by  $a_{ph}(440)$ , but appeared to coincide with maximal UV pigment expression.

2002). MAAs are potentially a source of highly chromophoric DOM and have been shown to be exuded from phytoplankton cells in culture (Vernet and Whitehead 1996) and to be present in CDOM in coastal waters (Whitehead and Vernet 2000). Release of MAAs by *Trichodesmium* has been demonstrated upon disaggregation of colonies (Subramaniam et al. 1999). Phytoplankton in near-surface thin layers in coastal waters have also been shown to contribute to CDOM in situ (Twardowski and Donaghay 2001). Given the ubiquitous nature of MAA production in phytoplankton spe-

cies and the potentially high UV radiation exposure in surface waters, exuded UV pigments might be a source of the CDOM increase observed by Twardowski and Donaghay (2001). The lack of direct evidence for MAA contribution to CDOM, such as a peak or shoulder in absorption spectra, does not necessarily negate their potential contribution. MAAs can be present in CDOM with no discernible features in the absorption spectra (Whitehead and Vernet 2000). Recent work suggests that spectral CDOM absorption is not simply the result of absorption by individual chromophores (Del Vecchio and Blough 2002). This more complex model of CDOM absorption could account for the absence of discernible MAA features in measured absorption spectra. Bacterial remediation of released UV pigments might also be important. Zooplankton in the open ocean have been shown to release CDOM (Steinberg et al. in press) and could play an important role in linking the production of UV-absorbing compounds and of CDOM in the open ocean, both by releasing phytoplankton cell contents and active transport of DOM from surface to deeper waters (Steinberg et al. 2000). It is interesting to note that a peak in the monthly averaged  $a_{\text{CDOM}}$  for both surface (<50 m) and deeper waters occurs during the period of maximal UV pigment expression at the surface, suggesting either a direct link or similar physical forcing of the two (Fig. 7).

The presence of UV-absorbing compounds in optically clear oligotrophic oceans might be important to organisms at higher trophic levels. MAAs have been shown to bioaccumulate in zooplankton and their consumers (Karentz et al. 1991; Whitehead et al. 2001) and might act as sunscreens in these organisms as well. Diel migration of zooplankton, swimming to the surface at night to feed, is common and occurs at the BATS site (e.g., Madin et al. 2001). This migration could act as a behavioral mechanism to reduce UV radiation damage, making the accumulation of MAAs unnecessary. It is still possible that bioaccumulation might occur in these organisms, as has been demonstrated in laboratory-raised Antarctic krill, a migrating species (Newman et al. 2000). MAAs might play an important role in mediating UV damage in zooplankton, which do not migrate to depth during the day and remain in the UV-rich surface waters.

Our results suggest that UV-absorbing pigments might be prevalent throughout the world's oceans and could play an important role in protecting phytoplankton and higher organisms in surface waters. They also might be a significant source of highly colored dissolved organic matter in the open oceans. Details of the geographic distribution, chemical nature, and production and loss rates of these UV-absorbing pigments require further study.

## References

- ALLALI, K., A. BRICAUD, M. BABIN, A. MOREL, AND P. CHANG. 1995. A new method for measuring spectral absorption coefficients of marine particles. *Limnol. Oceanogr.* **40**: 1526–1532.
- ANDERSON, R. A., R. R. BIDIGARE, M. D. KELLER, AND M. LATASA. 1996. A comparison of HPLC pigment signatures and electron microscopic observations for oligotrophic waters of the North Atlantic and North Pacific oceans. *Deep-Sea Res. II* **43**: 517–518.
- BANDARANAYAKE, W. M. 1998. Mycosporines: Are they nature's sunscreens? *Nat. Prod. Rep.* **15**: 159–172.
- BRICAUD, A., A. MOREL, AND L. PRIEUR. 1983. Optical efficiency factors of some phytoplankters. *Limnol. Oceanogr.* **28**: 816–832.
- CLEVELAND, J. S., AND A. D. WEIDEMANN. 1993. Quantifying absorption by aquatic particles: A multiple scattering correction for glass-fibre filters. *Limnol. Oceanogr.* **38**: 1321–1327.
- COCKELL, C. S., AND J. KNOWLAND. 1999. Ultraviolet radiation screening compounds. *Biol. Rev. Camb. Philos. Soc.* **74**: 311–345.
- CULLEN, J. J., AND M. P. LESSER. 1991. Inhibition of photosynthesis by ultraviolet radiation as a function of dose and dosage rate: Results for a marine diatom. *Mar. Biol.* **111**: 183–190.
- DEL VECCHIO, R., AND N. V. BLOUGH. 2002. Photobleaching of chromophoric dissolved organic matter in natural waters: Kinetics and modeling. *Mar. Chem.* **78**: 231–253.
- DURAND, M. D., AND R. J. OLSON. 1996. Contributions of phytoplankton light scattering and cell concentration changes to diel variations in beam attenuation in the equatorial Pacific from flow cytometric measurements of pico-, ultra- and nanoplankton. *Deep-Sea Res.* **43**: 891–906.
- , ———, AND S. W. CHISHOLM. 2001. Phytoplankton population dynamics at the Bermuda Atlantic Time-series station in the Sargasso Sea. *Deep-Sea Res. II, Topical Stud. Oceanogr.* **48**: 1983–2003.
- , R. E. GREEN, H. M. SOSIK, AND R. J. OLSON. 2002. Diel variations in optical properties of *Micromonas pusilla* (prasinophyceae). *J. Phycol.* **38**: 1132–1142.
- GARCIA-PICHEL, F. 1994. A model for internal self-shading in planktonic organisms and its implications for the usefulness of ultraviolet sunscreens. *Limnol. Oceanogr.* **39**: 1704–1717.
- GREEN, S. A., AND N. V. BLOUGH. 1994. Optical-absorption and fluorescence properties of chromophoric dissolved organic-matter in natural-waters. *Limnol. Oceanogr.* **39**: 1903–1916.
- HANNACH, G., AND A. C. SIGLEO. 1998. Photoinduction of UV-absorbing compounds in size species of marine diatom. *Mar. Ecol. Prog. Ser.* **174**: 207–222.
- KARENTZ, D., F. S. MCEUEN, M. C. LAND, AND W. C. DUNLAP. 1991. Survey of mycosporine like amino acids compounds in Antarctic marine organisms: Potential protection from ultraviolet exposure. *Mar. Biol.* **108**: 157–166.
- KLISCH, M., AND D.-P. HADER. 2000. Mycosporine-like amino acids in the marine dionoflagellate *Gyrodinium dorsum*: Induction by ultraviolet radiation. *J. Photochem. Photobiol. B* **55**: 178–182.
- . 2002. Wavelength dependence of mycosporine-like amino acid synthesis in *Gyrodinium dorsum*. *J. Photochem. Photobiol. B* **66**.
- KNAP, A. H., AND OTHERS. 1997. BATS methods manual. Version 4. U.S. JGOFS Planning Office.
- KRABS, G., K. BISCHOF, D. HANELT, U. KARSTEN, AND C. WIENCKE. 2002. Wavelength-dependent induction of UV absorbing mycosporine-like amino acids in the red alga *Chondrus crispus* under natural solar radiation. *J. Exp. Mar. Biol. Ecol.* **268**: 69–82.
- KROTKOV, N., J. R. HERMAN, P. K. BHARTIA, V. FIOLETOV, AND Z. AHMAD. 2001. Satellite estimation of spectral surface UV irradiance; 2. Effects of homogeneous clouds and snow. *J. Geophys. Res.* **106**: 11,743–11,759.
- LAURION, I., A. LAMI, AND R. SOMMARUGA. 2002. Distribution of mycosporine-like amino acids and photoprotective carotenoids among freshwater phytoplankton assemblages. *Aquat. Microb. Ecol.* **26**: 293–294.
- MADIN, L. P., E. F. HORGAN, AND D. K. STEINBERG. 2001. Zooplankton at the Bermuda Atlantic Time-series Study (BATS) station: Diel, seasonal, and interannual variation in biomass, 1994–1998. *Deep-Sea Res. II* **48**: 2063–2082.
- MITCHELL, B. G. 1990. Algorithms for determining the absorption

- coefficient of aquatic particulates using the quantitative filter technique (QFT). *SPIE* **1302**: 137–148.
- , AND OTHERS. 2000. Determination of spectral absorption coefficients of particles, dissolved material, and phytoplankton for discrete water samples. In G. S. Fargion and J. L. Mueller [eds.], *Ocean optics protocols for satellite ocean color sensor validation, revision 2*, NASA Technical Memorandum 2000-209966. National Aeronautics and Space Administration.
- MOISAN, T. A., AND B. G. MITCHELL. 2001. UV absorption by mycosporine-like amino acids in *Phaeocystis antarctica* Karsten induced by photosynthetically available radiation. *Mar. Biol.* **138**: 217–227.
- MOREL, A., AND A. BRICAUD. 1981. Theoretical results concerning light absorption in a discrete medium, and application to specific absorption of phytoplankton. *Deep-Sea Res.* **28**: 1375–1393.
- NEALE, P. J., A. T. BANASZAK, AND C. R. JARRIEL. 1998a. Ultra-violet sunscreens in *Gymnodinium sanguineum* (Dinophyceae): Mycosporine-like amino acids protect against inhibition of photosynthesis. *J. Phycol.* **34**: 928–938.
- , J. J. CULLEN, AND R. F. DAVIS. 1998b. Inhibition of marine photosynthesis by ultraviolet radiation: Variable sensitivity of phytoplankton in the Weddell-Scotia confluence during the austral spring. *Limnol. Oceanogr.* **43**: 433–448.
- , R. F. DAVIS, AND J. J. CULLEN. 1998c. Interactive effects if ozone depletion and vertical mixing on photosynthesis of Antarctic phytoplankton. *Nature* **392**: 585–589.
- NELSON, N. B., AND D. A. SIEGEL. 2002. Chromophoric DOM in the open ocean, p. 547–578. In D. A. Hansell and C. A. Carlson [eds.], *Biogeochemistry of marine dissolved organic matter*. Academic Press.
- , ———, AND A. F. MICHAELS. 1998. Seasonal dynamics of colored dissolved material in the Sargasso Sea. *Deep-Sea Res.* **I 45**: 931–957.
- NEWMAN, S. J., W. C. DUNLAP, S. NICOL, AND D. RITZ. 2000. Antarctic krill (*Euphausia superba*) acquire a UV-absorbing mycosporine-like amino acid from dietary algae. *J. Exp. Mar. Biol. Ecol.* **255**: 93–110.
- ORCUTT, K. M., AND OTHERS. 2001. A seasonal study of the significance of N-2 fixation by *Trichodesmium* spp. at the Bermuda Atlantic Time-series Study (BATS) site. *Deep-Sea Res.* **II, Topical Stud. Oceanogr.** **48**: 1583–1608.
- RICCHIAZZI, P., S. YANG, C. GAUTIER, AND D. SOWLE. 1998. SBDART: A research and teaching software tool for plane-parallel radiative transfer in the Earth's atmosphere. *Bull. Am. Meteorol. Soc.* **79**: 2101–2114.
- RIEGGER, L., AND D. ROBINSON. 1997. Photoinduction of UV-absorbing compounds in Antarctic diatoms and *Phaeocystis antarctica*. *Mar. Ecol. Prog. Ser.* **160**: 13–25.
- ROZEMA, J., AND OTHERS. 2002. The role of UV-B radiation in aquatic and terrestrial ecosystems—an experimental and functional analysis of the evolution of UV-absorbing compounds. *J. Photochem. Photobiol. B* **66**: 2–12.
- SHICK, J. M., AND W. C. DUNLAP. 2002. Mycosporine-like amino acids and related gadusols: biosynthesis, accumulation, and UV-protective functions in aquatic organisms. *Annu. Rev. Physiol.* **64**: 223–262.
- SHINA, R. P., M. KLISCH, E. W. HELBLING, AND D.-P. HADER. 2001. Induction of mycosporine-like amino acids (MAAs) in cyanobacteria by solar ultraviolet-B radiation. *J. Photochem. Photobiol. B* **60**: 129–135.
- SIEGEL, D. A., AND T. D. DICKEY. 1987. Observations of the vertical structure of the diffuse attenuation coefficient spectrum. *Deep-Sea Res.* **34**: 547–563.
- , A. F. MICHAELS, J. C. SORENSEN, M. C. O'BRIEN, AND M. A. HAMMER. 1995. Seasonal variability of light availability and utilization in the Sargasso Sea. *J. Geophys. Res.* **100**: 8695–8713.
- , S. MARITORENA, N. B. NELSON, D. A. HANSELL, AND M. LORENZI-KAYSER. 2002. Global distribution and dynamics of colored dissolved organic and detrital organic materials. *J. Geophys. Res.* **107**: 3228.
- SIMPSON, J. A., AND E. S. C. WEINER [EDS.]. 1989. *Oxford English dictionary*, 2nd ed. Clarendon Press.
- SMITH, R. C., AND K. S. BAKER. 1979. Penetration of UV-B and biologically effective dose-rates in natural waters. *Photochem. Photobiol.* **29**: 311–323.
- , ———, O. HOLM-HANSEN, AND R. S. OLSON. 1980. Photoinhibition of photosynthesis in natural waters. *Photochem. Photobiol.* **31**: 585–592.
- , AND OTHERS. 1992. Ozone depletion: Ultraviolet radiation and phytoplankton biology in Antarctic waters. *Science* **255**: 952–959.
- STEINBERG, D. K., C. A. CARLSON, N. R. BATES, S. A. GOLDTHWAIT, L. P. MADIN, AND A. F. MICHAELS. 2000. Zooplankton vertical migration and the active transport of dissolved organic and inorganic carbon in the Sargasso Sea. *Deep-Sea Res.* **I 47**: 137–158.
- , ———, R. J. JOHNSON, A. F. MICHAELS, AND A. H. KNAP. 2001. Overview of the US JGOFS Bermuda Atlantic Time-series Study (BATS): A decade-scale look at ocean biology and biogeochemistry. *Deep-Sea Res.* **II, Topical Studies in Oceanography** **48**: 1405–1447.
- , N. B. NELSON, AND C. A. CARLSON. In press. Production of chromophoric dissolved organic matter (CDOM) in the open ocean by zooplankton and colonial *Trichodesmium* spp. *Mar. Ecol. Prog. Ser.*
- SUBRAMANIAM, A., E. J. CARPENTER, D. KARENTZ, AND P. G. FALKOWSKI. 1999. Bio-optical properties of the marine diazotrophic cyanobacteria *Trichodesmium* sp. I. Absorption and photosynthetic action spectra. *Limnol. Oceanogr.* **44**: 608–617.
- TARTAROTTI, B., I. LAURION, AND R. SOMMARUGA. 2001. Large variability in the concentration of mycosporine-like amino acids among zooplankton from lakes located across an altitude gradient. *Limnol. Oceanogr.* **46**: 1546–1552.
- TWARDOWSKI, M. S., AND P. L. DONAGHAY. 2001. Separating in situ and terrigenous sources of absorption by dissolved materials in coastal waters. *J. Geophys. Res. Oceans* **106**: 2545–2560.
- VASILKOV, A., N. KROTKOV, J. HERMAN, C. MCCLAIN, K. ARRIGO, AND W. ROBINSON. 2001. Global mapping of underwater UV irradiances and DNA-weighted exposures using Total Ozone Mapping Spectrometer and Sea-viewing Wide Field-of-view Sensor data products. *J. Geophys. Res.* **106**: 27,205–27,219.
- VERNET, M., AND K. WHITEHEAD. 1996. Release of ultraviolet-absorbing compounds by the red tide dinoflagellate *Lingulodinium polyedrum*. *Mar. Biol.* **127**: 35–44.
- VINCENT, W. F., AND P. J. NEALE. 2000. Mechanisms of UV damage to aquatic organisms, p. 149–176. In S. de Mora, S. Demers, and M. Vernet [eds.], *The effects of UV radiation in the marine environment*. Cambridge Univ. Press.
- WHITEHEAD, K., AND M. VERNET. 2000. Influence of mycosporine-like amino acids (MAAs) on UV absorption by particulate and dissolved organic matter in La Jolla Bay. *Limnol. Oceanogr.* **45**: 1788–1796.
- , D. KARENTZ, AND J. I. HEDGES. 2001. Mycosporine-like amino acids (MAAs) in phytoplankton, a herbivorous pteropod (*Limacina helicina*), and its pteropod predator (*Clione antarctica*) in McMurdo Bay, Antarctica. *Mar. Biol.* **139**: 1013–1019.
- WHITEHEAD, R. F., S. J. DE MORA, AND S. DEMERS. 2000. Enhanced UV radiation—a new problem for the marine environment, p. 1–34. In S. de Mora, S. Demers, and M. Vernet [eds.], *The effects of UV radiation in the marine environment*. Cambridge environmental chemistry series. Cambridge Univ. Press.

Received: 12 February 2003

Accepted: 13 August 2003

Amended: 26 August 2003